Ab initio study of He(^1S)+Cl_2($X\ ^1\Sigma_g$,$^3\Pi_u$) potential energy surfaces

Grzegorz Chałasiński
Department of Chemistry and Biochemistry, Southern Illinois University, Carbondale, Illinois 62901 and Department of Chemistry, University of Warsaw, Pasteura 1, 02-093 Warszawa, Poland

Maciej Gutowski
Department of Chemistry, University of Utah, Salt Lake City, Utah 84112

M. M. Szczęśniak
Department of Chemistry, Oakland University, Rochester, Michigan 48309

Joanna Sadlej
Department of Chemistry, University of Warsaw, Pasteura 1, 02-093 Warszawa, Poland

Steve Scheiner
Department of Chemistry and Biochemistry, Southern Illinois University, Carbondale, Illinois 62901

(Received 2 May 1994; accepted 5 July 1994)

The potential energy surface of the ground state He+Cl_2($^1\Sigma_g$) is calculated by using the perturbation theory of intermolecular forces and supermolecular Møller–Plesset perturbation theory approach. The potential energy surface of the first excited triplet He+Cl_2($^3\Pi_u$) was evaluated using the supermolecular unrestricted Møller–Plesset perturbation theory approach. In the ground state two stable isomers are found which correspond to the linear He–Cl–Cl structure (a primary minimum, D_e=45.1 cm^{-1}, R_e=4.25 Å) and to the T-shaped structure with He perpendicular to the molecular axis (a secondary minimum, D_e=40.8 cm^{-1}, R_e=3.5 Å). The small difference between these geometries is mainly due to the induction effect which is larger for the linear form. The results obtained for the T-shaped minimum are in good agreement with the excitation spectroscopy experiments which observed only the T-shaped form [Beneventi *et al.*, J. Chem. Phys. **98**, 178 (1993)]. In the lowest triplet states correlating with Cl_2($^3\Pi_u$), $^3A'$ and $^3A''$, the same two isomers correspond to minima. Now, however, the T-shaped form is lower in energy. The $^3A'$ and $^3A''$ states correspond to (D_e,R_e) of (19.9 cm^{-1}, 3.75 Å) and (30.3 cm^{-1}, 3.50 Å), respectively, whereas the linear form is characterized by (19.8 cm^{-1}, 5.0 Å). The binding energy for the T form in the lower $^3A''$ state is in good agreement with the experimental value of Beneventi *et al.*

I. INTRODUCTION

According to experimental findings, two different forms of rare-gas–halogen molecule complexes exist: a linear form and a T-shaped form. The linear form is adopted by the Ar–ClF[1] and Kr–ClF complexes[2] whereas the Rg–X_2 systems (where X stands for a halogen atom) were found to be T shaped, e.g., He–I_2,[3] He–Cl_2,[4] He–Br_2,[5] Ne–Cl_2,[6] Ne–Br_2,[7] and Ar–Cl_2.[8] Understanding the origin of these shapes as well as reliable characterization and modeling of the potential energy surfaces (PES) for such systems has proven to be a challenge for experimentalists and theoreticians alike.

The *ab initio* calculations for the Ar–ClF dimer[9,10] agreed with the experimental finding that the linear isomer should be stable.[1] However, the calculations predicted the linear form to be stable also in the Ar–Cl_2 case[9,11] while the experimental measurements, using excitation spectroscopy[8] and microwave spectroscopy,[12] unambiguously detected *only* the T-shaped isomer. The energy difference between these two structures proved to be relatively small. Although the first estimates amounted to 30–36 cm^{-1},[9] more extensive calculations recently provided a better estimate of about 15 cm^{-1}.[11] One plausible reason why only the T-shaped isomer is observed is, according to Tao and Klemeperer,[9] that the zero-point energy of the linear form should be larger than that of the T-shaped form. In view of the small energy difference obtained in Ref. 11 it is conceivable that the *T* isomer of Ar–Cl_2 is stabilized by the smaller zero-point energy in this configuration.

Owing to Tao and Klemperer[9] and to our own recent results,[11] a better understanding of the discrepancy between theory and experiment in the Ar–Cl_2 case has been achieved. However, more detailed and quantitative study of the origin of the interaction and sources of anisotropy in the Rg–Cl_2 complexes is still needed.

The first question is whether in all Rg–Cl_2 complexes the T-shaped isomer is stable only because of the zero-point oscillations, or perhaps Ar–Cl_2 is an exception and some of the other complexes simply reveal a deeper well for the *T* structure. The best candidate to be different from Ar–Cl_2 is He–Cl_2 because a small difference between *L* and *T* forms in Ar–Cl_2 proved to be due to the induction effect[11] (the T-shaped isomer would be more stable than the linear if one neglected the induction contributions). The induction effect should be considerably reduced for He, due to its compact electron charge density and much smaller polarizability than Ar.

Another interesting issue is the stable structure of Rg–Cl_2 in the lowest triplet *B* excited state which correlates with the ^3B($^3\Pi_{0^+u}$) state of Cl_2. This state is used in the excitation spectroscopy experiments to produce the ground state Rg–Cl_2 molecules. The experiment has proven that the

 0021-9606/94/101(8)/6800/10/$6.00 © 1994 American Institute of Physics

Downloaded 09 Jun 2011 to 129.123.124.169. Redistribution subject to AIP license or copyright; see http://jcp.aip.org/about/rights_and_permissions

T-shaped isomer is stable.[4(b)] But is the excited state T shaped due to the deeper well depth or again due to zero-point oscillations?

This paper addresses the above two issues in the particular case of the He–Cl_2 complex. The potential energy surfaces and their components are calculated *ab initio* for both the ground He+$Cl_2(^1\Sigma_g)$ and excited He+$Cl_2(^3\Pi_u)$ states.

In the case of the ground state, the total interaction energy can be partitioned into fundamental components, such as electrostatic, exchange, induction and dispersion, by applying the combination of the supermolecular Møller–Plesset perturbation theory (MPPT)[13–15] with the perturbation theory of intermolecular forces.[16–19] Such an approach has proven successful in similar analyses of a number of other Ar-molecule van der Waals species.[20,21]

In the case of the excited state we analyzed both the $^3A'$ and $^3A''$ states which arise after removal of Π degeneracy for the T and all skew shapes. We neglected the spin–orbit splitting which was assumed to be geometry independent.

The experience with supermolecular calculations of weak interactions between closed and open shell species is very limited. In the case of atom–diatom interactions one should mention two recently studied models, Ar–OH($^2\Pi$,$^2\Sigma$)[22] and B(^3P)–$H_2(^1\Sigma_g)$[23] which are relevant to our complex. These studies applied CI-type methods. In the present case we use unrestricted MPPT(UMPPT) which has been shown reliable and accurate previously, in the case of $^3\Pi$ MgHe and $^3\Sigma$ He_2.[24]

II. METHOD AND DEFINITIONS

The supermolecular Møller–Plesset perturbation theory (MPPT) interaction energy corrections are derived as the difference between the values for the total energy of the dimer and the sum of the subsystem energies, in every order of perturbation theory

$$\Delta E^{(n)}=E_{AB}^{(n)}-E_A^{(n)}-E_B^{(n)}, \quad n=\mathrm{SCF},2,3,4,\ldots \tag{1}$$

The sum of corrections through the nth order will be denoted $\Delta E(n)$; thus, e.g., $\Delta E(3)$ will symbolize the sum of ΔE^{SCF}, $\Delta E^{(2)}$, and $\Delta E^{(3)}$.

Each individual $\Delta E^{(n)}$ correction can be interpreted[13–15] in terms of intermolecular Møller–Plesset perturbation theory (I-MPPT) which encompasses all well-defined and meaningful contributions to the interaction energy such as electrostatic, induction, dispersion, and exchange, and may be expressed in the form of a double perturbation expansion.[17–19] The I-MPPT interaction energy corrections are denoted $\epsilon^{(ij)}$, where i and j refer to the order of the intermolecular interaction operator and the intramolecular correlation operator, respectively (see Ref. 17 for more details).

A. Partitioning of ΔE^{SCF}

ΔE^{SCF} can be dissected as follows (cf. Refs. 13–15 for more details):

$$\Delta E^{\mathrm{SCF}}=\Delta E^{\mathrm{HL}}+\Delta E_{\mathrm{def}}^{\mathrm{SCF}}, \tag{2}$$

$$\Delta E^{\mathrm{HL}}=\epsilon_{\mathrm{es}}^{(10)}+\epsilon_{\mathrm{exch}}^{\mathrm{HL}}, \tag{3}$$

where ΔE^{HL} and $\Delta E_{\mathrm{def}}^{\mathrm{SCF}}$ are the Heitler–London and SCF-deformation contributions, respectively. ΔE^{HL} is further divided into the electrostatic, $\epsilon_{\mathrm{es}}^{(10)}$, and exchange, $\epsilon_{\mathrm{exch}}^{\mathrm{HL}}$, components. The SCF deformation originates from mutual electric polarization restrained by the Pauli principle (quantum exchange effects).[25] In this sense, the SCF deformation energy may be considered as *quantum induction effect*. Two exchangeless approximations to $\Delta E_{\mathrm{def}}^{\mathrm{SCF}}$ are also considered here, which are $\epsilon_{\mathrm{ind}}^{(20)}$ and $\epsilon_{\mathrm{ind},r}^{(20)}$ and may be viewed as two representations of *classic induction effect*. The former describes the second-order induction effect at the uncoupled Hartree–Fock (UCHF) level, and the latter at the coupled Hartree–Fock (CHF) level ("r" denotes inclusion of response effects).[26]

B. Partitioning of $\Delta E^{(2)}$

$$\Delta E^{(2)}=\epsilon_{\mathrm{es},r}^{(12)}+\epsilon_{\mathrm{disp}}^{(20)}+\Delta E_{\mathrm{def}}^{(2)}+\Delta E_{\mathrm{exch}}^{(2)}. \tag{4}$$

$\epsilon_{\mathrm{es},r}^{(12)}$ denotes the second-order electrostatic correlation energy with response effects[14] and $\epsilon_{\mathrm{disp}}^{(20)}$ the second-order Hartree–Fock dispersion energy. $\Delta E_{\mathrm{def}}^{(2)}$ and $\Delta E_{\mathrm{exch}}^{(2)}$ stand for the second-order deformation correlation correction to the SCF deformation and the second-order exchange correlation, respectively. The latter encompasses the exchange–correlation effects related to electrostatic correlation and dispersion and can be approximated as follows (provided the deformation-correlation contribution is negligible):[14]

$$\Delta E_{\mathrm{exch}}^{(2)}\cong\Delta E^{(2)}-\epsilon_{\mathrm{disp}}^{(20)}-\epsilon_{\mathrm{es},r}^{(12)}. \tag{5}$$

C. Partitioning of $\Delta E^{(3)}$

$$\Delta E^{(3)}=\epsilon_{\mathrm{disp}}^{(21)}+\epsilon_{\mathrm{disp}}^{(30)}+\epsilon_{\mathrm{es},r}^{(13)}+\Delta E_{\mathrm{def}}^{(3)}+\Delta E_{\mathrm{exch}}^{(3)}. \tag{6}$$

$\epsilon_{\mathrm{es},r}^{(13)}$ denotes the third-order electrostatic correlation energy with response effects,[14,15] $\epsilon_{\mathrm{disp}}^{(30)}$ represents the third-order Hartree–Fock dispersion energy, while $\epsilon_{\mathrm{disp}}^{(21)}$ describes the first-order intracorrelation correction to the second-order dispersion energy.[17] $\Delta E_{\mathrm{def}}^{(3)}$ and $\Delta E_{\mathrm{exch}}^{(3)}$ stand for the third-order deformation correlation correction and the second-order exchange correlation, respectively. The first term in Eq. (6) is the dominant component of the $\Delta E^{(3)}$ correction in Ar-molecule complexes.

D. Excited state case

The excited states of He–Cl_2 are open shell states which are calculated by means of UMPPT. The supermolecular energies are defined identically as in Eq. (1) by replacing the restricted Hartree–Fock and correlated energies by unrestricted ones. However, the decomposition into perturbation components is more involved and has not been done so far.

The fact that the UMPPT states are not pure spin states is not a serious problem as long as the contamination is small and *identical* for both the dimer and the monomer case. A typical problem is that not only may the UHF procedure have problems with convergence but may converge to a local minimum of different spin contamination for the dimer than that for the monomers. Such an inconsistency may lead to nonsensical interaction energies. Applying a projected ap-

Downloaded 09 Jun 2011 to 129.123.124.169. Redistribution subject to AIP license or copyright; see http://jcp.aip.org/about/rights_and_permissions

proach did not appear to be a remedy. Another problem worth mentioning is the Hartree–Fock instability due to symmetry breaking.[27]

E. Calculations of interaction energies

Calculations of all the supermolecular ΔE values and perturbational interaction terms $\epsilon^{(ij)}$ are performed using the basis set of the entire complex, i.e., dimer-centered basis sets (DCBSs).[28–30] With reference to supermolecular quantities this procedure amounts to applying the counterpoise method of Boys and Bernardi.[31] To assure the consistency of evaluation of the MPPT and I-MPPT interaction energy corrections of all the intermolecular perturbation terms, $\epsilon^{(ij)}$ must be derived in the DCBS as well.

In contrast to weak interactions between closed-shell states, the counterpoise procedure is not so clear-cut for interactions involving open-shell states. For example, calculation for the Π symmetry Cl_2 monomers with ghost orbitals located as in the T-shaped geometry may provide an unphysical splitting into A' and A'' states. The question is: shall we use separate monomer counterpoise states for separate A' and A'' dimer states? Or, perhaps, the consistent treatment of monomers demands that we use the same monomer wave functions for both states. In either case the presence of ghost orbitals breaks the monomer symmetry. In addition, the splitting results in quasidegeneracy, the more serious the smaller BSSE. In this work we use the second approach (cf. also Esposti and Werner).[22] Another solution has been suggested by Alexander.[23] Nevertheless the problem is worth further studies.

F. Basis sets and geometries

The basis sets used throughout this study were based on the following choice: Cl: $(14s,10p,4d,1f)/[7s,5p,2d,1f]$ medium-polarized basis set constructed in Ref. 32 according to the prescription of Sadlej,[33] augmented with one f-symmetry orbital (exponent 0.15); the performance of this basis set for the Cl_2 molecule was discussed previously for Ar–Cl_2 (see Table 1 in Ref. 11).

For He the $(10s,6p,2d)/[6s,4p,2d]$ basis set was used. The $(10s6p)/[6s4p]$ part was taken from Gutowski *et al.*[34] (this set was used there in the $HeLi^+$ case). The d-symmetry functions (exponents: 0.152 93, 0.498 71) were optimized for the dispersion term by Gutowski *et al.*[35] This basis set, denoted $spdf$, was used to derive the PES.

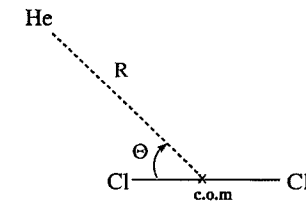

FIG. 1. Definition of geometrical parameters of the He–Cl_2 complex.

Selected points on the PES were also calculated with a larger basis set, denoted $spdf(b\text{-}ext)$ which included a set of bond functions $[3s3p2d]$ of Tao and Pan[36] (sp: 0.9,0.3,0.1; d: 0.6,0.2). This set was originally designed for He_2 but has also proven very efficient in Ar_2 calculations as well as for other complexes with Ar.[37] The role of bond functions has been investigated also in Refs. 35 and 38.

The definition of geometrical parameters of the He–Cl_2 complex is shown in Fig. 1. R denotes the distance between the center of mass of the Cl_2 molecule and the He atom, and Θ corresponds to the angle between the R vector and the Cl_2 bond axis. The interatomic separation in the ground $^1\Sigma_g^+$ state of Cl_2 was fixed at 1.990 Å and in the $^3\Pi_u$ state at 2.400 Å.[39] The excited Cl_2 molecule is in the lowest triplet state and thus accessible within the UMPPT framework. Moreover, this state is well isolated from the ground and other excited states so no curve crossing occurs. The spin contamination is very small and S^2 amounts to 2.0427. The optimization of geometry within the UMP4/$spdf$ treatment yielded $R_e=2.471a_0$ to be compared with the experimental value of $2.396a_0$ and the *ab initio* estimate of $2.43a_0$.[39]

The calculations were carried out using GAUSSIAN 88[40] and GAUSSIAN 92[41] programs and the intermolecular perturbation theory package of Cybulski.[42]

III. RESULTS AND DISCUSSION OF GROUND STATE OF He–$Cl_2(1\Sigma_g^+)$

A. Features of total PES

The PES (Table I) reveals two minima: a global one for the linear configuration (at $\Theta=0.0°$ and reflected by symme-

TABLE I. Interaction energies in the ground state He–$Cl_2(\Sigma_g^+)$ complex from the MP2/$spdf$ level calculations in μH.

	Θ (deg): 0.0	20.0	40.0	60.0	80.0	90.0
R (Å)						
3.00	...	...	...	...	368.43	130.71
3.25	...	...	...	...	−1.32	−99.50
3.50	1340.2	1581.6	1109.1	267.71	−106.97	−145.14
3.75	205.50	379.63	302.30	16.00	−117.74	−131.12
4.00	−115.90	−8.97	19.97	−60.38	−99.95	−103.62
4.25	−167.50	−106.50	−62.50	−72.20	−77.62	−77.80
4.50	−144.20	−110.39	−74.28	−63.48	−51.99	−57.36
4.75	−109.06	−90.21	−64.57	−50.48	−43.19	−42.20

Downloaded 09 Jun 2011 to 129.123.124.169. Redistribution subject to AIP license or copyright; see http://jcp.aip.org/about/rights_and_permissions

TABLE II. Energy characteristics (in μH) of the two minima of the ground state He–$Cl_2(\Sigma_g^+)$ complex (frozen-core approximation).

	Linear (R=4.25 Å, Θ=0°)		T (R=3.5 Å, Θ=90°)	
	spdf	*spdf*(*b*-ext)	*spdf*	*spdf*(*b*-ext)
ΔE^{SCF}	112.10	110.91	110.09	110.99
$\Delta E^{(2)}$	−279.66	−297.70	−255.33	−274.35
$\Delta E(2)$	−167.56	−186.79	−145.14	−163.37
$\Delta E^{(3)}$		7.49		0.67
$\Delta E^{(4)}$		−26.20		−23.00
$\Delta E(4)$		−205.50		−185.70
ϵ_{exch}^{HL}	177.31	175.60	153.57	154.38
$\epsilon_{es}^{(10)}$	−35.97	−35.53	−30.90	−30.74
ΔE_{def}^{SCF}	−29.24	−29.16	−12.57	−12.65
$\epsilon_{ind}^{(20)}$	···	−22.45	···	−8.00
$\epsilon_{ind,r}^{(20)}$	−27.01	−26.95	−8.88	−8.90
$\epsilon_{es,r}^{(12)}$	−5.76	−6.22	−8.56	−9.08
$\epsilon_{disp}^{(20)}$	−305.60	−324.94	−290.91	−311.77
$\Delta E_{exch}^{(2)}$	31.7	33.46	44.24	46.50
$\epsilon_{disp}^{(21)}$	4.1	1.67	1.34	−1.5
$\Delta E^{SCF}+\epsilon_{disp}^{(20)}$	−193.5	−214.03	−180.82	−200.78
$\Delta E^{HL}+\epsilon_{disp}^{(20)}$	−164.26	−184.87	−168.24	−188.13

try at 180°) and a local one for the T configuration (Θ =90.0°). The estimates of the equilibrium distances for the linear and T configurations at the MP4/*spdf* level are 4.25 and 3.50 Å, respectively (see Tables II and III). They are expected to be somewhat too large because the *spdf* basis set underestimates attraction.

In order to visualize the shape of the PES, the curves representing cuts across the PES (obtained at the MP2/*spdf* level of theory) at eight values of R: 3.0, 3.25, 3.50, 3.75, 4.0, 4.25, 4.50, and 4.75 Å, and for Θ from 0° to 180° are shown in Fig. 2 and Table I.

One can see that the T minimum region closely approaches the middle of the Cl–Cl bond and is located between steeply repulsive walls. These walls serve as a considerable barrier for internal rotation of the Cl_2 moiety around its center of mass. The linear minimum, although deeper in an absolute sense, occurs at larger $R\approx$4.25 Å in a relatively flatter region of the PES. There, a barrier for the internal rotation of Cl_2 is only about 20 cm^{-1}. The barrier for the lowest energy path from L to T amounts to 20 cm^{-1} and corresponds to a transition state at around R=4.5 Å and

TABLE III. Characteristics (in μH) of the minimum regions of the ground state He–$Cl_2(\Sigma_g^+)$ complex. Basis set was *spdf* unless stated otherwise.

R (Å)	MP2	SCF+D	MP4	MP4[a]
		T configuration		
3.25	−99.5	−180.0	−125.8	
3.50	−145.1	−180.0	−163.6	−185.7
3.75	−131.1	−147.4	−143.8	
		Linear configuration		
4.00	−115.9	−183.1	−137.3	
4.25	−167.5	−193.5	−183.2	−205.5
4.50	−144.2	−153.8	154.9	

[a]Basis set *spdf*(*b*-ext), i.e., *spdf*+bond(3*s*3*p*2*d*).

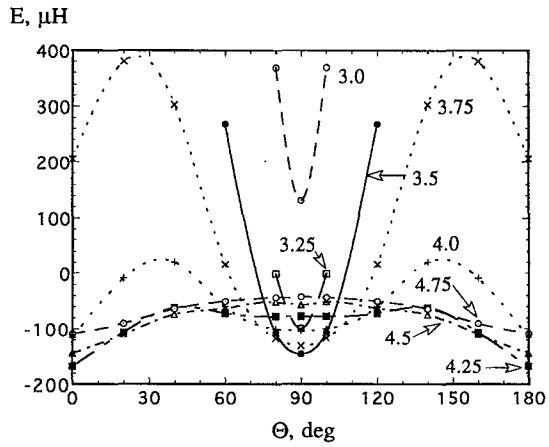

FIG. 2. Potential energy surface of the ground-state He–$Cl_2(X\ ^1\Sigma_g)$ complex.

Θ=40°. All the above numerical values in Table I should be considered as approximate as the *spdf* basis set provides results that are not attractive enough by ~10% and additional unsaturation is caused by neglecting the higher order correlation effect.

The energetic characteristics of the two minima are presented in Tables II and III. To examine convergence with respect to the basis set effects, the analysis is performed for the *spdf*, and *spdf*(*b-ext*) basis sets. The best estimates of D_e at the global and local minima are 45.0 and 40.7 cm^{-1}, respectively, obtained with the *spdf*(*b-ext*) basis set. In Tables II and III one can see that the linear minimum persists as deeper than the T minimum at each level of theory [$\Delta E(2)$,$\Delta E(4)$,SCF+disp] and for each basis set [*spdf*, and *spdf*(*b-ext*)], and the difference at the MP4 level remains within the range of 3–5 cm^{-1}.

As expected, for both minima a major stabilizing factor is dispersion. What distinguishes them is the role of the induction effect. Indeed, the ratio $\Delta E_{def}^{SCF}/\epsilon_{disp}^{(20)}$ obtained using the *spdf*(*b-ext*) amounts to 9% for the linear structure and only 4% for T, which may be compared to 13% and 3%, respectively, in the Ar–Cl_2 case.[11] That is, the induction effect favors the linear structure of He–Cl_2, although not to the same degree as in the case of the complex with Ar (the compact electronic charge density of He yields less polarization effect than does Ar). Even stronger relative stabilization of the analogous linear minimum by induction has been observed previously for Ar–ClF[10] and Ar–HCl.[43] For the collinear Ar–Cl–F configuration ΔE_{def}^{SCF}, compared with $\epsilon_{disp}^{(20)}$, represents a larger contribution and amounts to 23% of the latter, whereas for the T configuration it amounts to only 3%. For the collinear hydrogen-bonded Ar–H–Cl configuration, the relative induction contribution is still larger, about 30% of the dispersion term.

To estimate the quality of our D_e values it is important to analyze the convergence of MPPT and the basis set effects. The convergence through the fourth order is similar to that for Ar–ClF[10] and Ar–HCl[43] as well as other van der Waals complexes of argon.[44] That is, $\Delta E^{(2)}$ provides a major attrac-

Downloaded 09 Jun 2011 to 129.123.124.169. Redistribution subject to AIP license or copyright; see http://jcp.aip.org/about/rights_and_permissions

TABLE IV. Θ dependence of the interaction energy contributions of the ground state He–$Cl_2(\Sigma_g^+)$ complex calculated with the *spdf* basis set (frozen-core approximation, R=4.25 Å, energies in μH).

Θ (deg)	$\epsilon_{es}^{(10)}$	ϵ_{exch}^{HL}	ΔE^{HL}	ΔE^{SCF}	ΔE_{def}^{SCF}	$\epsilon_{ind,r}^{(20)}$	$\epsilon_{disp}^{(20)}$	$\epsilon_{es,r}^{(12)}$	$\Delta E^{(2)}$	$\Delta E_{exch}^{(2)}$	$\Delta E(2)$
0	−35.97	177.31	141.34	112.10	−29.24	−27.01	−305.60	−5.76	−279.66	31.70	−167.56
20	−41.16	210.18	169.02	142.07	−26.95	−21.90	−278.22	−6.29	−248.58	35.92	−106.51
40	−30.81	164.49	133.68	116.88	−16.80	−11.53	−205.29	−5.49	−179.37	31.41	−62.49
60	−11.74	64.23	52.49	46.39	−6.10	−3.89	−131.27	−2.88	−118.61	15.54	−72.22
80	−2.68	14.16	11.47	10.21	−1.26	−0.80	−91.59	−1.09	−87.83	4.85	−77.62
90	−1.71	8.69	6.98	6.24	−0.74	−0.48	−86.68	−0.86	−84.04	3.50	−77.80

tive contribution, $\Delta E^{(3)}$ is much smaller and repulsive, and $\Delta E^{(4)}$ is attractive and dominated by triple excitations terms. Moreover, $\Delta E^{(2)}$ and $\Delta E^{(3)}$ are dominated by dispersion components ($\epsilon_{disp}^{(20)}$ and $\epsilon_{disp}^{(21)}$, respectively), and the same is expected for $\Delta E^{(4)}$. What is different is the role of $\Delta E^{(3)}$ which is negligibly small here. Interestingly, this pattern of convergence is also somewhat different from that in such He complexes as He_2,[45] He–H_2O,[46] He–CO_2,[47] He–NO^-,[48] where the $\Delta E^{(3)}$ correction is *attractive* and *quite important*. It appears that the latter behavior is typical for complexes involving atoms from the first and second period. In contrast, those including the third-period atoms reveal repulsive $\Delta E^{(3)}$ corrections which are canceled by the attractive $\Delta E^{(4)}$ terms. It seems that the complexes involving both types of atoms, such as He–Cl_2, show intermediate behavior.

It is reasonable to assume that through the fourth order, the correlation effects are already accurately reproduced. For the *spdf* basis, the most important deficiency is the basis set unsaturation of the dispersion contribution. As to the *spdf(b-ext)* basis set, it provides almost saturated description of the dispersion effect although a small error is due to unsaturation of the intramonomer correlation effects. Whereas it is not possible to accurately calculate this error, one may use a vast body of evidence collected for Ar-molecule complexes to obtain a reasonable estimate. According to this evidence (see Refs. 43 and 37), the *spdf* basis gives a 15%–30% error. Application of an extended set of bond functions [basis set *spdf(b-ext)*] provides results only ±5% in error.

B. Sources of anisotropy of PES

An angular scan of the PES, and its components for the primary minimum (R=4.25 Å), is shown in Table IV and in Figs. 3 and 4.

The HL-exchange term (Fig. 3) displays a strong angular dependence with a minimum at 90° and maxima at 20° and 160°. Toward the Cl ends (Θ=0° and 180°), ϵ_{exch}^{HL} decreases. This indicates some depletion of the diffuse part of electron density at Θ=0° and 180°, similar to the Cl ends of HCl and ClF, but far less pronounced. This feature is also reflected by the electrostatic term, $\epsilon_{es}^{(10)}$, which is of purely charge-overlap character in the present case and shows distinct flattening at the molecular axis. Consequently, the electron distribution of ground state $Cl_2(^1\Sigma_g^+)$ may be visualized as a dumbbell with slight indentations at the ends.

It is interesting to compare this view with the description of the Cl_2 charge distribution inferred from the study of Ar–Cl_2.[11] As shown in Ref. 11, probing Cl_2 with Ar has revealed the Cl_2 charge distribution of a dumbbell with flattened ends. This is entirely consistent with the present conclusions that there exist slight indentations at the ends of the dumbbell. In view of its smaller van der Waals radius the He atom can access the indentations while Ar cannot. The He

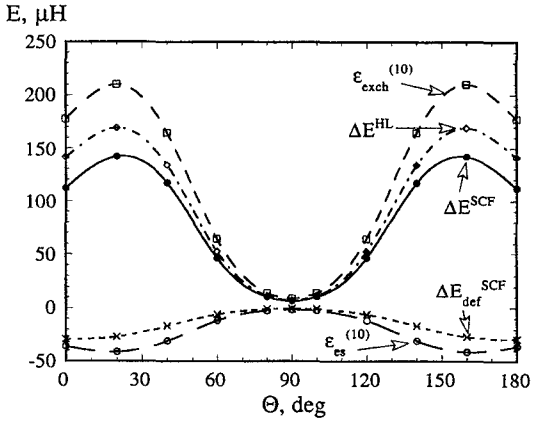

FIG. 3. Θ dependence of the SCF interaction energy and its components in the ground-state He–Cl_2 complex (R=4.25 Å).

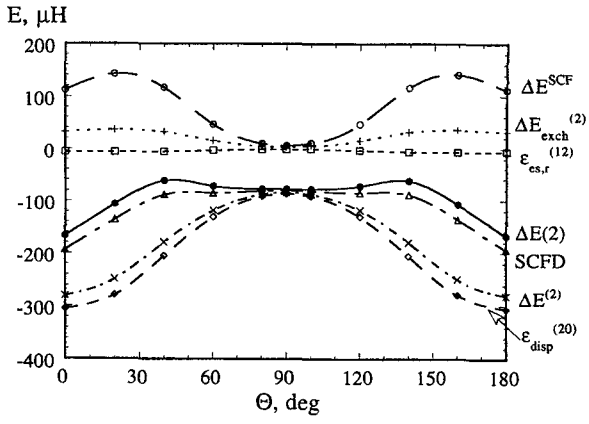

FIG. 4. Θ dependence of the correlated interaction energy components in the ground-state He–Cl_2 complex (R=4.25 Å).

Downloaded 09 Jun 2011 to 129.123.124.169. Redistribution subject to AIP license or copyright; see http://jcp.aip.org/about/rights_and_permissions

TABLE V. Potential energy surface of the excited state $^3A'$ He–Cl_2($^3\Pi_u$) complex from the UMP2/*spdf* level calculations in μH.

	Θ (deg)					
R (Å)	0.0	20.0	40.0	60.0	80.0	90.0
3.25						13.29
3.50	a	a	a	215.49	−58.53	−78.33
3.75	a	a	502.93	1.94	−85.75	−91.74
4.00	a	a	98.01	−58.31	−78.89	−79.79
4.25	278.7	a	−32.80	−65.12	−63.69	−62.79
4.50	9.97	a	−62.86	−56.08	−49.07	−47.75
4.75	−67.43	−69.01	−59.80	−44.34	−37.28	−36.12
5.00	−77.48	−67.94	−48.40	−34.10	−28.32	−27.46
5.25	−67.06	a	−37.22	−29.94	−21.64	−15.85
5.50	−52.91					

[a]Convergence problems.

atom may thus be considered a more sensitive probe of the electron distribution.[46]

The details of the anisotropies of $\Delta E_{\rm def}^{\rm SCF}$ and $\epsilon_{{\rm ind},r}^{(20)}$ (not shown) are largely similar and the latter faithfully approximates the former.

The correlation components are shown in Fig. 4 along with the total interaction energy. One can see that $\Delta E^{(2)}$ is actually determined by the dispersion term. $\epsilon_{{\rm es},r}^{(12)}$ is practically negligible, while $\Delta E_{\rm exch}^{(2)}$ is small. The $\Delta E^{(2)}$ and $\epsilon_{\rm disp}^{(20)}$ curves reveal minima at the Cl ends and a maximum in the middle of the Cl–Cl bond. One notes that the dispersion term favors the linear configuration whereas the *T* minimum occurs at the lowest value of the repulsive $\epsilon_{\rm exch}^{\rm HL}$ term (see above and Fig. 3). The above description agrees with the findings for the Ar–Cl_2 case.[11]

The total interaction energy $\Delta E(2)$, at *R* fixed at 4.25 Å, shown in Fig. 4, gives us the shape of the PES in the region of the linear minimum. For angles close to the *T* configuration, the curve corresponds to that portion of the PES which is related to distances substantially larger than the *T* equilibrium distance (R=3.5 Å). In this region the PES looks like a wide plateau which lies above the *L* minimum region. On closer look the plateau reveals small barriers at its borders, 40° and 140°, and a tiny barrier in the middle. It should be noted that the border barriers occur for a wide range of intermolecular distances, as they separate the *L*-minimum valley from the *T*-minimum valley (see also Fig. 2).

For very large *R* (not shown in the figures) the shape is determined by the dispersion component. That is, it has valleys at the Cl ends whereas the plateau for the *T* configuration transforms into a barrier.

IV. RESULTS AND DISCUSSION OF EXCITED $^3A'$ AND $^3A''$ STATES OF He–Cl_2

The He–Cl_2 clusters studied by pump–probe spectroscopy correlate with the long-lived Cl_2 *B* $^3\Pi_{0+u}$ state.[49,50] If we neglect spin–orbit coupling, this state corresponds to the lowest triplet state, $^3\Pi_u$, with the dominant electronic configuration $(\sigma_g)^2(\pi_u)^4(\pi_g)^3(\sigma_u)^1$.[39] The latter is a single excited configuration from the ground state configuration $(\sigma_g)^2(\pi_u)^4(\pi_g)^4(\sigma_u)^0$. Because of the presence of the He atom the symmetry of the complex is lower than that of Cl_2. Therefore, unless He–Cl_2 assumes a strictly linear geometry, two nondegenerate electronic states arise related to the original $^3\Pi_u$ state of Cl_2. More specifically, if the geometry of the complex is $C_{\infty v}$, the $^3\Pi_u$ state of Cl_2 correlates with the $^3\Pi$ state of He–Cl_2. If the geometry is C_{2v}, the $^3\Pi_u$ state gives rise to $^3A_1$ and $^3B_1$ states, which are, respectively, symmetric and antisymmetric with respect to the plane of the cluster. For the intermediate skew geometries of the C_s symmetry, these two states are termed $^3A'$ and $^3A''$. The states are expected to be very close to each other since the perturbation exerted by He is small. In addition, when He rotates from the perpendicular T-shaped geometry toward the collinear structure these two states converge to become degenerate at the linear geometry. It is important to note here that we do not know how these two electronic states are involved in the experimentally produced excited ^3B He–Cl_2 clusters.

Application of the UMPPT method to states which are so close must cause convergence problems (cf. Ref. 27). Below we describe how we obtained an almost complete scan of the PES for $^3A'$ and a fragment of the $^3A''$ PES related to the perpendicular configuration

$^3A'$: The convergence to the $^3A'$ state was smooth for the *T*-shaped geometry. For the neighboring skewed geometries, convergence was only possible by initializing the SCF procedure with the vectors from the perpendicular geometry. Further geometries were converged by using vectors from some other converged nearby geometries. The reported points on the PES in the range of Θ=90°–Θ=40° were obtained in this way. For Θ=20° only two points (R=4.75 Å and R=5.0 Å) were obtained. For other *R* distances we were not able to force convergence by using the vectors from neighboring geometries. It is plausible that the two states, $^3A'$ and $^3A''$, are already too close to each other in this geometry and the symmetry breaking prevented the procedure from converging.

In the collinear geometry where the Π state degeneracy was exact, the convergence was smooth in the region of 4.25 Å–5.0 Å, provided that the initial guess was obtained by diagonalization of the core Hamiltonian. The points where the convergence failed are indicated by letter "*c*" in Table V.

In all the calculations described above the spin contamination of both the Cl_2 moiety (calculated within DCBS) and

Downloaded 09 Jun 2011 to 129.123.124.169. Redistribution subject to AIP license or copyright; see http://jcp.aip.org/about/rights_and_permissions

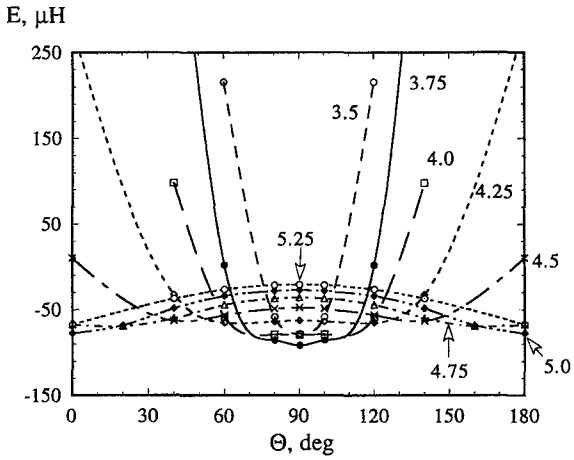

FIG. 5. Potential energy surface of the $^3A'$ excited state He–Cl_2 ($^3\Pi_u$) complex.

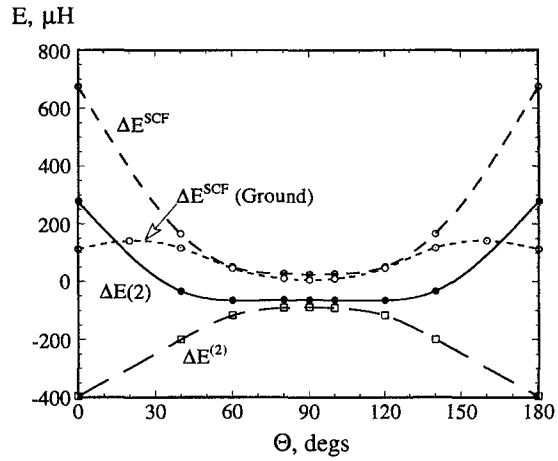

FIG. 6. Θ dependence of the UMPPT interaction energy and its components in the $^3A'$ excited state He–Cl_2 ($^3\Pi_u$) complex at R=4.25 Å. The ground-state SCF interaction energy curve corresponding to R=4.25 Å is included for comparison.

in the dimer was very small. For the Cl_2 monomer S^2 was equal to 2.0427 for the MCBS and all DCBS calculations. For the dimer S^2 oscillated from 2.0423 to 2.0429. Occasionally the UHF procedure for the dimer converged to an unwanted local minimum. This was manifested by S^2 different from the above values and equal to 2.0197. It is important to stress that both the dimer and monomer must have practically the same spin contamination. Otherwise subtraction of the dimer and monomer energies becomes inconsistent and the interaction energies nonsensical.

$^3A''$: The $^3A''$ state was calculated only for the T-shaped geometry for R ranging from 3.50 to 5.25 Å. Convergence of the UHF procedure was achieved by starting from the vectors from the RHF calculations and switching one electron from the highest occupied a_2 orbital to the lowest virtual b_2 orbital. The resulting vectors were used to converge the remaining points. As in the $^3A'$ state the spin contamination proved to be very small with S^2 equal to 2.0427. To evaluate the interaction energies, the same monomer energies (calculated with DCBS) were used as for the A' state. We also estimated that the difference between the DCBS energies for the ghost orbitals located in the A' and A'' symmetries did not exceed a few μH.

A. Features of total $^3A'$ PES

The PES of the excited $^3A'$ state reveals two minima: a global one for the T configuration (Θ=90.0°) and a local one for the linear configuration (at Θ=0.0° and reflected by symmetry at 180°). The estimates of the equilibrium distances for the L and T configurations at the UMP2/*spdf* level are 5.0 and 3.75 Å, respectively. In contrast to the ground state, the T-shaped form constitutes a deeper minimum (see below).

In order to visualize the shape of the PES, the curves representing cuts across the PES (obtained at the UMP2/*spdf* level of theory) at eight values of R and for Θ=0° −180° are shown in Fig. 5 and Table V. As noted above, at some points in Table V (the entries denoted c) we were unable to converge the UHF procedure.

One can see that the T minimum region relatively closely approaches the middle of the Cl–Cl bond and is located between steeply repulsive walls. These walls hinder the internal rotation of the Cl_2 moiety around its center of mass. In contrast to the ground state case, the T minimum is deeper than the L minimum. The linear minimum occurs at larger $R\approx5.0$ Å, in a relatively flatter region of the PES. There, a barrier for the internal rotation of Cl_2 is only about 11.0 cm^{-1}. The barrier for the lowest energy path from T to L amounts to 6 cm^{-1} and corresponds to a transition state at around R=4.5 Å and Θ=40°.

To examine convergence with respect to the basis set extension we attempted to use the basis set augmented with bond functions, *spdf(b-ext)*. For the linear isomer a reasonable lowering of 1 cm^{-1} (which constitutes ~7%) was obtained. Such lowering is compatible with the results for the ground state and is typical of other complexes.[37] However, at the T configurations the bond functions resulted in breaking of symmetry and led to a dramatic and improbable lowering of 9 cm^{-1}, i.e., about 45%!

It is difficult to establish precisely the accuracy of the excited state results. First, the calculations are not as elaborate as for the ground state and the basis set lacked bond functions. Moreover, experience with van der Waals complexes in excited states is extremely limited and there is not much evidence which can guide us in this regard. Yet, the *ab initio* calculations for model systems, $^3\Sigma$ state of He_2 and $^3\Pi$ state of MgHe, which used a similar strategy, provided D_e results which were too small by less than 10%.[24] To be on the safe side we assume that our present results are at least semiquantitatively correct and certainly warrant further studies.

B. Sources of anisotropy of $^3A'$ PES

For an open shell state we are not able to perform a similar decomposition of the interaction energy as for closed shell states. However, one can still analyze the major parts: the total SCF contribution and the total correlation contribu-

Downloaded 09 Jun 2011 to 129.123.124.169. Redistribution subject to AIP license or copyright; see http://jcp.aip.org/about/rights_and_permissions

TABLE VI. Θ dependence of the UMPPT interaction energy contributions in the $^3A'$ state of He–$Cl_2(^3\Pi_u)$ complex in *spdf* basis set (frozen-core approximation; R=4.75 Å; energies in μH).

Θ (deg)	ΔE^{SCF}	$\Delta E^{(2)}$	$\Delta E(2)$
0	109.34	−176.77	−67.43
20	71.37	−140.38	−69.02
40	26.23	−86.03	−59.80
60	9.40	−53.74	−44.34
80	7.39	−44.67	−37.28
90	7.22	−43.34	−36.12

TABLE VIII. Comparison of the interaction energies for the ground and the $^3A'$ and $^3A''$ excited states of the T-shaped He–Cl_2 complex in the van der Waals minimum region (R=3.75 Å) through the fourth order of UMPPT (energies in μH).

	$^1A'$	$^3A'$	$^3A''$
ΔE^{SCF}	42.8	111.7	49.2
$\Delta E(2)$	−131.1	−91.7	−119.9
$\Delta E(3)$	−129.0	−83.1	−121.1
$\Delta E(4)$	−143.8	−90.5	−132.3

tion. In the case of He–molecule interactions, the SCF part is very well approximated by the total Heitler–London interaction energy and reflects the behavior of the exchange component (the induction effect is small for He complexes). In the second order, the $\Delta E^{(2)}$ term is closely related to the dispersion term while the exchange components are small. Consequently, from the anisotropies of the SCF and second-order interaction energies we can infer the behaviors of the HL-exchange and dispersion energies, respectively. The anisotropies of these two terms at R=4.25 Å are visualized in Fig. 6 and in Table VI (R=4.75 Å). One can see that the behavior of the SCF curve is distinctly different from that of the ground state in Fig. 3. The ground state ΔE^{SCF} possesses a maximum around Θ=20° indicating indentation in the electron charge density at the Cl end (Θ=0°). In the excited state there is no such maximum and the curve rises fairly sharply (see Fig. 6 where the ground-state SCF curve for R=4.25 Å is included for comparison). It should be mentioned that the Cl–Cl bond distance is larger in the excited state which contributes to the observed sharp maximum in the excited-state SCF curve at Θ=0°.

Concluding, the electron density of the excited $^3A'$ state at the Cl end has an ellipsoidal convex shape. In contrast, the ground state density reveals in the analogous region a concave shape. Therefore, whereas the ground state Cl_2 may be viewed as a dumbbell with flattened, concave ends, the excited-state Cl_2 is a stretched dumbbell with convex ends.

Different shapes of ground and excited electron charge distributions may be rationalized in terms of the configurations that correspond to these states. The ground state configuration is $(\sigma_g)^2(\pi_u)^4(\pi_g)^4(\sigma_u)^0$. The relative flattening of the density at the Cl end may be attributed to the excess of π contributions (which have nodes on the interatomic axis) over the axially symmetric σ (which are of ellipsoidal shape). In the excited state one electron is promoted from a π_g orbital to σ_u and the resulting configuration is: $(\sigma_g)^2(\pi_u)^4(\pi_g)^3(\sigma_u)^1$. Consequently, the excited state has an enhanced σ contribution which favors more charge density at the axis and at the Cl ends.

C. PES of the $^3A''$ state

We have calculated the $^3A''$ state interaction energies only for the T-shaped isomer. Rotation of He toward the linear structure gradually reduces the splitting between A' and A'' states until they become degenerate for Θ=0°.

The UMPPT interaction energies for different R, derived in the *spdf* basis set, are listed in Table VII. The van der Waals minimum results obtained at the UMP4/*spdf* level are shown in Table VIII. It is seen that the A'' PES lies below the A' PES. Our best estimate of D_e is 30.3 cm^{-1}, obtained at the UMP4/*spdf* level of theory for R_e=3.50 Å. At the same level the A' well depth amounted to 19.9 cm^{-1} at R=3.75 Å, some 10 cm^{-1} less. Because of problems with symmetry breaking we were unable to augment the *spdf* basis set with bond functions.

It should be noted that the A'' state has a different character than the A' state. There are two reasons for the lowering of the interaction energy of the A'' state with respect to

TABLE VII. R dependence of the UMPPT interaction energy contributions for the T-shaped configuration in the $^3A'(^3A_1)$ and $^3A''(^3B_1)$ excited states of He–$Cl_2(^3\Pi_u)$ complex in *spdf* basis set (in μH).

	$^3A'(^3A_1)$			$^3A''(^3B_1)$		
R (Å)	ΔE^{SCF}	$\Delta E^{(2)}$	$\Delta E(2)$	ΔE^{SCF}	$\Delta E^{(2)}$	$\Delta E(2)$
3.25	529.52	−516.23	13.29	291.74	−343.79	−52.04
3.50	243.51	−321.84	−78.33	120.66	−240.45	−119.80
3.75	111.68[a]	−203.43	−91.74[b]	49.21[c]	−169.13	−119.92[d]
4.00	51.79	−131.57	−79.79	19.79	−119.78	−100.00
4.25	25.02	−87.82	−62.79	7.83	−85.57	−77.73
4.50	13.00	−60.75	−47.75	3.03	−61.75	−58.71
4.75	7.22	−43.34	−36.12	1.13	−45.07	−43.94
5.00	4.03	−31.49	−27.46	0.39	−33.29	−32.90
5.25	2.04	−23.07	−21.03	0.11	−24.90	−24.79

[a]The CP-uncorrected result is 47.62 μH.
[b]The CP-uncorrected result is −660.50 μH.
[c]The CP-uncorrected result is −14.85 μH.
[d]The CP-uncorrected result is −688.68 μH.

Downloaded 09 Jun 2011 to 129.123.124.169. Redistribution subject to AIP license or copyright; see http://jcp.aip.org/about/rights_and_permissions

A'. First, the SCF energy is significantly reduced, and second, $\Delta E^{(3)}$ and $\Delta E^{(4)}$ are both attractive in the A'' state (while they cancel each other for the A' state). Interestingly, the $\Delta E^{(2)}$ energies are very similar in both cases.

It is difficult to rationalize the difference in ΔE^{SCF} energies for the A' and A'' states. Following Ref. 51 one could try to invoke the symmetry of overlapping orbitals to justify the difference in repulsion. However, all the orbitals which might make a difference [i.e., $\pi_g(a_2,b_2)$ and $\sigma_u(b_2)$] have zero overlap with the He $1s(a_1)$ orbital. Hence, the repulsive overlap-dependent part of $\epsilon_{\mathrm{exch}}^{\mathrm{HL}}$ is expected to be similar for the $^3A'$ and $^3A''$ states. Therefore, it is plausible that the origin of the difference is in the attractive components $\epsilon_{\mathrm{es}}^{(10)}$ or $\Delta E_{\mathrm{def}}^{\mathrm{SCF}}$. We prefer to postpone further speculations until the perturbation analysis of the SCF energy for open-shell systems is implemented.

More puzzling facts are left unanswered. For example, why are the $\Delta E^{(2)}$ terms almost equal in both cases? Perhaps, the dispersion energy, which dominates the excited state correlation energy is very isotropic. Much more difficult is rationalization of the reverse pattern of the third- and fourth-order terms in both states. It should be reiterated that the UMPPT convergence pattern in the A'' state is similar to the ground state and different from that in the A' state.

Finally, we wish to comment on the value of the CP correction in these calculations. Table VII includes some values which are not CP corrected (R=3.75 Å, Θ=90°). The uncorrected values are obviously nonsensical. The large magnitude of CP correction in this case is quite typical and results from the basis set which was chosen for the quality of interaction energy components and not to minimize BSSE. It should be stressed that the value of this correction should not be used to judge the quality of interaction energy.[52]

V. CONCLUSIONS

A. Ground state of He–Cl_2

Our analysis of the *ab initio* PES of the ground state of the He–Cl_2 (Σ_g^+) complex indicates a global minimum for the collinear L configuration and a local minimum for the T-shaped configuration. The estimates of R_e and D_e for these two minima are: (4.25 Å, 45.1 cm^{-1}) and (3.5 Å, 40.8 cm^{-1}). The obtained values of D_e are expected to be in error by ±5%. According to our findings the T configuration is confined by rather steep barriers to the bending motion, whereas in the L configuration Cl_2 can rotate nearly freely.

The experimental measurements of Beneventi *et al.*[4(c)] provide an estimate of R_e and D_e only for the T configuration, $R_e \approx 3.56$ Å and $D_e \approx 38.2$ cm^{-1}, in good agreement with the present results. The L configuration has so far eluded experimental detection. This is somewhat puzzling since the L configuration is found to be slightly more stable. However, according to the estimates of Tao and Klemperer for Ar–Cl_2[9] the zero-point energy may be different enough for these two isomers to make D_0 for the T-shape form larger. More likely, any complex as floppy as He–Cl_2 displays a complicated dynamics which should be treated in the way that goes beyond the simple harmonic approximation. The question as to which isomer is more stable should be resolved on dynamical grounds.

Our results shed new light also on the origin of anisotropy of the He–Cl_2 interaction. First, the electron distribution of the ground Σ_g^+ state Cl_2 may be visualized as a dumbbell. When He serves as a probe it can detect slight indentations at the Cl ends. In the previous study of Ar–Cl_2[11] the Ar atom acting as a probe detected distinct flattening at the ends. Second, the induction energy favors the L isomer. Indeed the HL+disp approximation predicts the T-shaped conformer to be more stable by about 1 cm^{-1}. The induction effect is relatively less important for the L isomer than in the Ar–Cl_2 case (it amounts to 9% and 4% of the dispersion energy for the L and T forms, respectively, whereas for Ar–Cl_2 this contribution was 12% and 3%, respectively).

In this context, it is worthwhile to emphasize the role of the induction term in determining relative stability of different isomers of van der Waals complexes containing halogens. While this term never provides a quantitatively dominant portion of binding energy its anisotropy may significantly influence the energetical balance and the final geometry.

B. $^3A'$ and $^3A''$ states of He–Cl_2

Both states possess two minima, a global one for the T structure and the local one for the linear geometry. This is in contrast to the ground state where the linear geometry corresponds to the deeper minimum. Of the two excited states $^3A''$ is deeper. The estimates of D_e and R_e for $^3A''$ are 30.3 cm^{-1} and 3.50 Å. These values obtained at the UMP4 level are still basis-set unsaturated and D_e may be viewed as a lower bound to the true values and R_e is expected to be overestimated. Because of symmetry both states coincide at the linear geometry. The well depth parameters obtained at the UMP4 level for this minimum are D_e=18.9 cm^{-1} and R_e=5.0 Å. Again, the D_e value is expected to be underestimated.

Our results shed new light also on the origin of anisotropy of the He–Cl_2 interaction. In particular, the electron distribution of the $^3\Pi_u$ excited state Cl_2 may be visualized as a dumbbell. In contrast to the ground state, however, this dumbbell seems to be stretched, with a longer "waist," and of convex rather than concave shape at the Cl ends. This difference may be attributed to promotion of an electron from a π-symmetry orbital to a σ orbital, thus enhancing the ellipsoidal shape of the electronic distribution. Unfortunately, at the present state of our decomposition scheme we were not able to separate the induction term to find out how its role has changed. Further studies of the excited state with complete dissection of the interaction energy are underway in this laboratory.

ACKNOWLEDGMENTS

This work was supported by the National Institutes of Health (No. GM36912) and by the Polish Committee for Scientific Research KBN Grant No. 2 0556 91 01. M.G. was supported by National Science Foundation (Grant No. CHE-9116286).

Downloaded 09 Jun 2011 to 129.123.124.169. Redistribution subject to AIP license or copyright; see http://jcp.aip.org/about/rights_and_permissions

[1] S. J. Harris, S. E. Novick, W. Klemperer, and W. E. Falconer, J. Chem. Phys. **61**, 193 (1974).
[2] S. E. Novick, S. J. Harris, K. C. Janda, and W. Klemperer, Can. J. Phys. **53**, 2007 (1975).
[3] R. E. Smalley, D. H. Levy, and L. Wharton, J. Chem. Phys. **64**, 3266 (1976).
[4] (a) J. I. Cline, D. D. Evard, F. Thommen, and K. C. Janda, J. Chem. Phys. **84**, 1165 (1986); (b) J. I. Cline, B. P. Reid, D. D. Evard, N. Sivakumar, N. Halberstadt, and K. C. Janda, *ibid.* **89**, 3535 (1988); (c) L. Beneventi, P. Casavecchia, G. G. Volpi, C. R. Bielar, and K. C. Janda, *ibid.* **98**, 178 (1993).
[5] L. J. van de Brught, J. P. Nicolai, and M. C. Heaven, J. Chem. Phys. **81**, 5514 (1984).
[6] D. D. Evard, F. Thommen, and K. C. Janda, J. Chem. Phys. **84**, 3630 (1986).
[7] F. Thommen, D. D. Evard, and K. C. Janda, J. Chem. Phys. **82**, 5259 (1985).
[8] D. D. Evard, J. I. Cline, and K. C. Janda, J. Chem. Phys. **88**, 5433 (1988).
[9] F.-M. Tao and W. Klemperer, J. Chem. Phys. **97**, 440 (1992).
[10] J. Sadlej, G. Chałasiński, and M. M. Szczęśniak, J. Chem. Phys. **99**, 3700 (1993).
[11] J. Sadlej, G. Chałasiński, and M. M. Szczęśniak, Theochem **307**, 187 (1994).
[12] Y. Xu, W. Jager, I. Ozier, and M. C. L. Gerry, J. Chem. Phys. **98**, 3726 (1993).
[13] G. Chałasiński and M. M. Szczęśniak, Mol. Phys. **63**, 205 (1988).
[14] (a) R. Moszyński, S. Rybak, S. M. Cybulski, and G. Chałasiński, Chem. Phys. Lett. **166**, 609 (1990); (b) S. M. Cybulski, G. Chałasiński, and R. Moszyński, J. Chem. Phys. **92**, 4357 (1990); S. M. Cybulski and G. Chałasiński, Chem. Phys. Lett. **197**, 591 (1992).
[15] G. Chałasiński, M. M. Szczęśniak, and S. M. Cybulski, J. Chem. Phys. **92**, 2481 (1990).
[16] K. Szalewicz and B. Jeziorski, Mol. Phys. **38**, 191 (1979).
[17] S. Rybak, B. Jeziorski, and K. Szalewicz, J. Chem. Phys. **95**, 6576 (1991).
[18] H. L. Williams, K. Szalewicz, B. Jeziorski, R. Moszynski, and S. Rybak, J. Chem. Phys. **98**, 1279 (1993).
[19] R. Moszyński, B. Jeziorski, and K. Szalewicz, Chem. Phys. **166**, 329 (1992).
[20] G. Chałasiński and M. M. Szczęśniak, Croat. Chem. Acta **65**, 17 (1992).
[21] M. M. Szczęśniak and G. Chałasiński, Theochem. **261**, 37 (1992).
[22] A. D. Esposti and H. J. Werner, J. Chem. Phys. **93**, 3351 (1990).
[23] M. H. Alexander, J. Chem. Phys. **99**, 6014 (1993).
[24] G. Chałasiński and J. Simons, Chem. Phys. Lett. **148**, 289 (1988).
[25] M. Gutowski and L. Piela, Mol. Phys. **64**, 943 (1988).
[26] S. M. Cybulski, J. Chem. Phys. **97**, 7545 (1992).
[27] J. H. van Lenthe and F. B. van Duijneveldt, J. Chem. Phys. **81**, 3168 (1984).
[28] J. H. van Lenthe, J. G. C. M. van Duijneveldt-van de Rijdt, and F. B. van Duijneveldt, Adv. Chem. Phys. **69**, 521 (1987).
[29] G. Chałasiński and M. Gutowski, Chem. Rev. **88**, 943 (1988).
[30] M. Gutowski and G. Chałasiński, J. Chem. Phys. **98**, 5540 (1993); M. Gutowski, J. G. C. M. van Duijneveldt-van de Rijdt, J. H. van Lenthe, and F. B. van Duijneveldt, J. Chem. Phys. **98**, 4728 (1993).
[31] S. F. Boys and F. Bernardi, Mol. Phys. **19**, 553 (1970).
[32] G. Chałasiński, S. M. Cybulski, M. M. Szczęśniak, and S. Scheiner, J. Chem. Phys. **91**, 7048 (1989).
[33] A. J. Sadlej, Coll. Czech. Chem. Commun. **53**, 1995 (1988).
[34] M. Gutowski, F. B. van Duijneveldt, G. Chałasiński, and L. Piela, Mol. Phys. **61**, 233 (1987).
[35] M. Gutowski, J. Verbeek, J. H. van Lenthe, and G. Chałasiński, Chem. Phys. **111**, 271 (1987).
[36] (a) F-M. Tao and Y-K. Pan, J. Chem. Phys. **97**, 4989 (1992); (b) F-M. Tao, J. Chem. Phys. **98**, 3049 (1992).
[37] G. Chałasiński and M. M. Szczęśniak, Chem. Rev. (submitted).
[38] (a) R. J. Vos, R. Hendriks, and F. B. van Duijneveldt, J. Comp. Chem. **11**, 1 (1990); (b) J. G. C. M. van Duijenveldt-van de Rijdt, and F. B. van Duijneveldt, *ibid.* **13**, 399 (1992); (c) R. J. Vos, J. H. van Lenthe, and F. B. van Duijneveldt, J. Chem. Phys. **93**, 643 (1990).
[39] S. Peyerimhoff and R. J. Buenker, Chem. Phys. **57**, 279 (1981).
[40] M. J. Frisch, M. Head-Gordon, H. B. Schlegel, K. Raghavachari, J. S. Binkley, C. Gonzales, D. J. Defrees, D. J. Fox, R. A. Whiteside, R. Seeger, C. F. Melius, J. Baker, R. L. Martin, L. R. Kahn, J. J. P. Stewart, E. M. Fluder, S. Topiol, and J. A. Pople, GAUSSIAN 88, Gaussian, Inc., Pittsburgh, PA, 1988.
[41] M. J. Frisch, G. W. Trucks, M. Head-Gordon, P. M. W. Gill, M. W. Wong, J. B. Foresman, B. G. Johnson, H. B. Schlegel, M. A. Robb, E. S. Replogle, R. Gomperts, J. L. Andres, K. Raghavachari, J. S. Binkley, C. Gonzales, R. L. Martin, D. J. Fox, D. J. Defrees, J. Baker, J. J. P. Stewart, and J. A. Pople, GAUSSIAN 92, Gaussian, Inc., Pittsburgh, PA, 1992.
[42] S. M. Cybulski, Trurl package, Carbondale, IL, 1991.
[43] G. Chałasiński, M. M. Szczęśniak, and B. Kukawska-Tarnawska, J. Chem. Phys. **94**, 6677 (1991).
[44] G. Chałasiński and M. M. Szczęśniak (unpublished results).
[45] J. Sauer, P. Hobza, P. Čarsky, and R. Zahradník, Chem. Phys. Lett. **134**, 553 (1987).
[46] B. Kukawska-Tarnawska, G. Chałasiński, and M. M. Szczęśniak, Theochem **297**, 313 (1993).
[47] J. Sadlej, Theochem **209**, 231 (1990).
[48] G. Chałasiński and B. Kukawska-Tarnawska, J. Phys. Chem. **94**, 3450 (1990).
[49] R. Moszyński, B. Jeziorski, and K. Szalewicz, Chem. Phys. **166**, 329 (1992).
[50] J. A. Coxon, J. Mol. Spectrosc. **82**, 264 (1980).
[51] S. Bililign, M. Gutowski, J. Simons, and W. H. Breckenridge, J. Chem. Phys. **100**, 8212 (1994).
[52] F. B. van Duijneveldt, J. G. C. M. van Duijneveldt-van de Rijdt, and J. H. van Lenthe, Chem. Rev. (submitted).

Downloaded 09 Jun 2011 to 129.123.124.169. Redistribution subject to AIP license or copyright; see http://jcp.aip.org/about/rights_and_permissions